Cavity Expansion and Fracture Propagation in Dunnville Sandstone

Originally written for the University of Minnesota Undergraduate Research Opportunities Program (UROP) Public Presentation Requirement

Jacob Sharpe

Professor Joseph F. Labuz, Adviser

Abstract

Fracture initiation of a pressurized circular cavity in Dunnville Sandstone was observed using a cavity expansion apparatus and particle tracking technique called digital image correlation. Different far-field stress configurations were used to determine its effect on the fracture initiation and propagation. The results of the tests show fracture initiation as a percent of the borehole breakdown (peak) pressure was determined to decrease as the far-field stress increased. In addition, the crack opening displacement at the borehole wall measured at peak pressure increased as the far-field stress increased.

Table of Contents

1.0 Introduction

A common technique to extract rock or other resources from the earth's surface is to excavate or drill a circular opening called a borehole, which can be used for site investigations, in-situ testing, and water, oil, or gas recovery. Depending on the state of stress and the strength, failure of the rock surrounding the borehole may lead to monetary losses, environmental damages, and possibly loss of life. Understanding how failure initiates and propagates in relation to rock type, existing stress, and borehole pressure can lead to more efficient and safer designs.

This research project focuses on the relationship between far-field stress, fracture initiation pressure, and fracture conditions. The rock used in the investigation is Dunnville sandstone, a porous soft rock. Experiments were carried out using a Cavity Expansion Apparatus (CEA), where far-field stress and borehole pressure are generated under controlled conditions. The experiments were monitored with a particle tracking technique called digital image correlation (DIC) to determine the displacement field. The failure process was tracked with DIC, and tensile fracture was identified as the failure mode, where the characteristics of the crack governed the displacement field.

2.0 Theory

The problem of an internally pressurized borehole can be modeled as a circular cavity in an infinite medium with no applied stress. From the simple failure criterion of Rankine (Hoek, 1983), it is found that the pressure in the borehole is equal to the tensile strength of the rock. When a far-field stress is applied, then the tensile strength, borehole pressure, and far-field stress (in one direction only) are related by the Kirsch solution with a pressurized cavity.

$$\sigma_t = \sigma_o + p$$

where p is the internal pressure of the cavity, σ_o is the far-field stress, and σ_t is the tensile strength of the rock.

Furthermore, a fracture can be described as thin ellipse, with the ratio of the major to minor axes on the order of 10^3 or greater. At the crack tip, a stress singularity exists and the intensity of the stress singularity is characterized by the stress intensity factor, K (Irwin 1958). The stress intensity factor can be found for three different modes of fracture: opening, sliding, and tearing. Mode I is opening, which is the fracture process in a cavity expansion test. A fracture will propagate when the stress intensity factor reaches a critical value, K_{IC}, which is called the fracture toughness.

$$K_{IC} = \sigma_c \sqrt{\pi a}\, f(\alpha)$$

where σ_c, is a critical stress, a is the radius of the borehole, and $f(a)$ is some function of the radius of the borehole. An inelastic region called the fracture process zone forms in the area of the crack tip due to the stress singularity. The length of the process zone can be determined from the methods used in this experiment (Labuz *et al*., 1985).

3.0 Experimental Setup

Cavity expansion tests consist of different components: specimen, cavity expansion apparatus, digital camera, and the correlation software.

3.1 Specimen

The specimen is a 100 x 100 x 100 mm cubic block of Dunnville sandstone (Fig. 1). All six faces were machine ground to ensure smooth, flat, and perpendicular surfaces. A diamond-tipped core barrel was used to create a 20 mm diameter borehole that was perpendicular to the bedding of the rock.

Figure 1: A cavity Expansion specimen with a borehole with a diameter of 20 mm that is drilled perpendicular to the bedding planes. The black and white speckle pattern is shown on the top of the specimen.

A speckle pattern was created on the surface perpendicular to the borehole for the DIC analysis. The speckle pattern consisted of white primer and paint on the sandstone's surface to have a white background, followed by black speckles applied by using black spray paint.

3.2 Cavity Expansion Apparatus

The cavity expansion apparatus (CEA) consists of the reaction frame, axial loading cell, and the urethane packer (Blanksma, 2013). The urethane packer is designed to pressurize the borehole without allowing fluid into the pores of the rock. The axial loading cell is used to house the specimen, and the reaction frame is used to house the axial loading cell.

The urethane packer consists of a straddle packer and a urethane sleeve. The urethane packer is approximately 190 mm long and 20 mm in diameter (Blanksma, 2013). Hydraulic fluid is pressurized from a manual hand pump and is injected from the straddle packer inside the urethane packer. The urethane sleeve keeps the fluid from exiting the packer and entering the pores of the specimen. Approximately 150 mm of the urethane packer is pressurized. The pressurized interval expands and acts on the borehole walls, allowing the rock to fracture at some pressure. Collar seals were used to stop leakage from the packer.

The axial loading cell consists of four 19 mm threaded rods that connect top and bottom platens. The bottom platen is 26 mm thick and has a 20 mm diameter hole cut out in the center for the urethane packer to fit through. The specimen sits on top of the bottom platen. Two 13 mm thick top platens are stacked one on top of the other. The first top platen is placed on top of the specimen and has a 100 x 65 mm rectangle cut out. A 13 mm thick glass platen 100 x 65 mm is placed inside the steel platen's cut out. This is done in order to capture images of the surface of the specimen for DIC. The second top platen is then placed on top of the first with a similar cut out. Four 98 x 97 mm side platens were placed in the axial loading cell where hydraulic flat-jacks can apply a stress on the platens. Hydraulic flat-jacks are two thin steel plates that are welded at the edges (Blanksma, 2013). This allows hydraulic fluid to be pumped into the flat-jacks to produce pressure on the side platens.

The reaction frame consists of four 50.8 mm thick, 381 mm diameter steel cylinders with a 203 mm square cut-out in the center. Each cylinder is stacked on top of the other creating a 203 x 203 x 203 mm cubic space for placement of the axial loading cell.

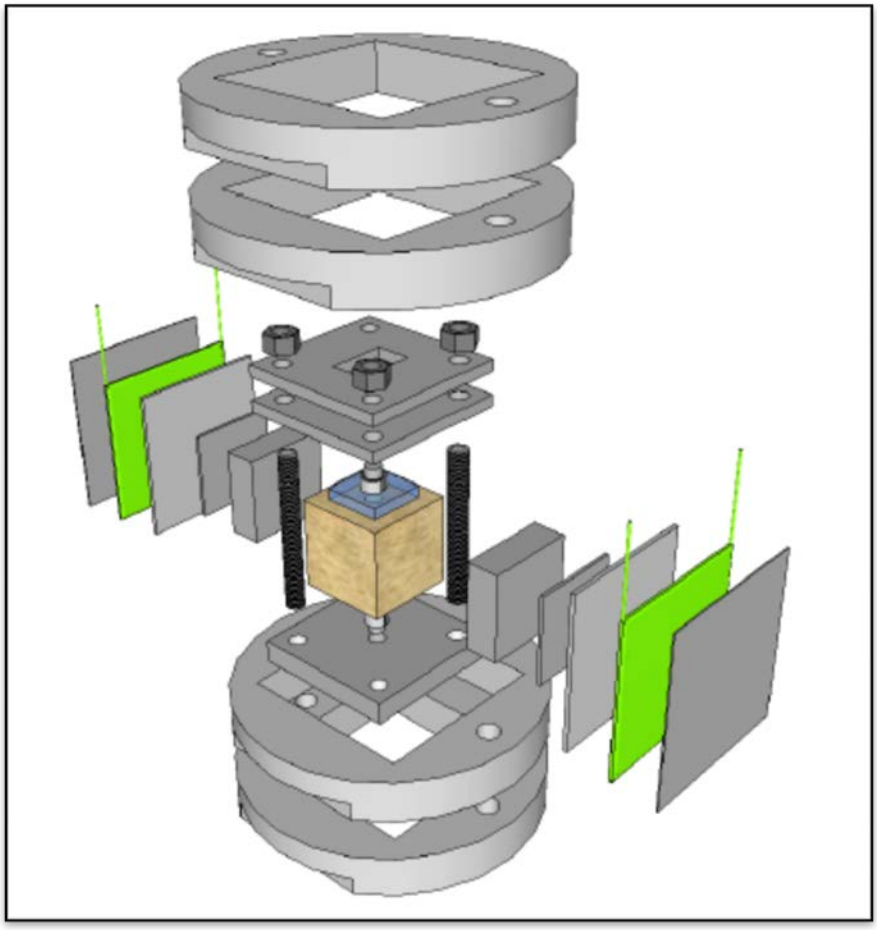

Figure 2: The cavity expansion apparatus in exploded view. The hydraulic flat jacks (green), glass platen (blue) and the rest of the platens and the reaction frame are shown (Blanksma, 2013).

3.3 Digital Image Correlation

Digital image correlation (DIC) is a particle tracking technique used to create displacement fields (Peters and Ranson, 1982). A high speed, high resolution, charge-coupled device camera is used to capture images of the speckled pattern surface of the specimen as the borehole is being pressurized. A PC was used to control the camera using a firewire interface software Unibrain fire-i 810b. This software allowed for control of resolution, capture rate, and allows for preview of the images.

Each image is comprised of pixels where the number of pixels per image depends on the resolution. Each pixel is assigned a grayscale value between 0-255 where lighter pixels have larger values than darker pixels. A group of pixels is called a subset.

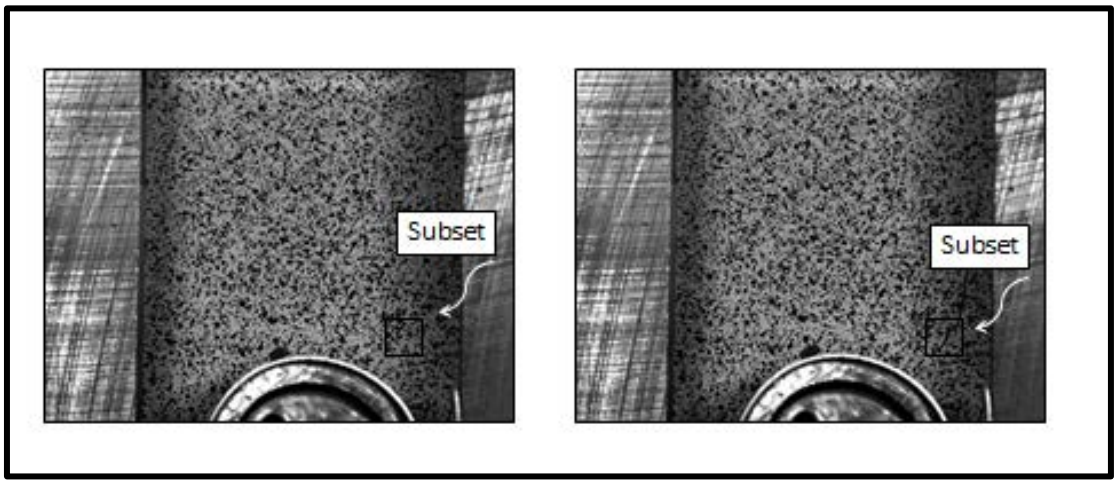

Figure 3: An undeformed image (left) and a deformed (right) of the specimen through the glass platen. A subset of a region of interest is shown and the difference between the two images are shown by the fracture in the right image that results in the movement of the speckles.

The DIC analysis was carried out using the commercial software DaVis. The software compares two images: a reference image (pre-deformation) and a current image (post deformation). The software compares each subset in the reference image and determines where it is in the current image within a region of interest. From the original and current positions, the displacement fields are generated.

3.4 Testing Configurations

The far-field stress was applied in the x-direction via the hydraulic flat-jacks. The top and bottom platens provide a plane strain condition in the z-direction. No stress is applied in the y-direction: this was done in order to know where the crack will form, which is normal to the minimum principal stress direction. Tests were performed at varying far-field stresses of 0.3, 0.5,

0.7, 0.9 MPa. These values were chosen as a result of the tensile strength determined from a Brazilian test. The tensile strength of Dunnville Sandstone was determined to be 1.7 MPa. These stresses were chosen in order to see the relationship between far-field stress and borehole breakdown pressure and fracture-initiation pressure. Fracture initiation and propagation were tracked with digital photos.

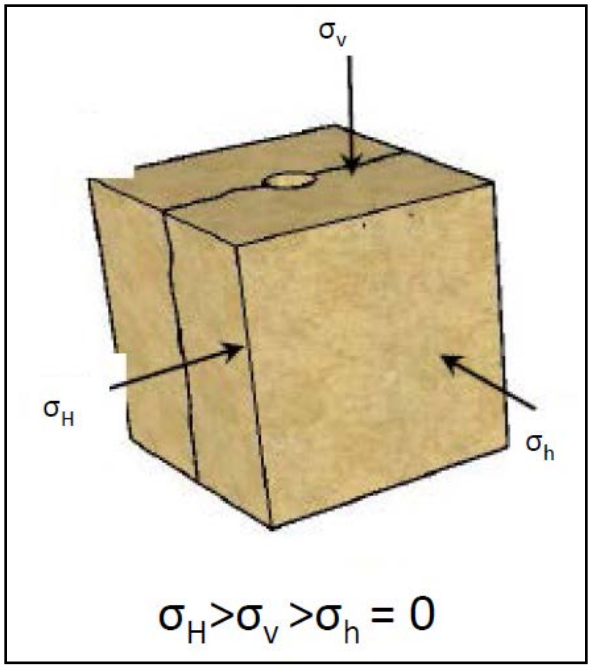

Figure 4: Diagram of the fracture orientation and loading configuration on the rock from the cavity expansion apparatus.

The packer was pressurized at a rate of approximately 1 cubic centimeter per minute. Since no fluid is entering the specimen, the rate at which fluid is injected into the packer does not affect the breakdown pressure (Zoback, 1977). Images were captured for DIC analysis at a rate of one frame per second. The images that were taken were two megapixels of 8-bit grayscale resolution.

4.0 Results and Analysis

Fracture initiation pressure was determined from the DIC analysis. Displacement contours consist of the surface displacement in the x-direction and y-direction. The white semicircle at the bottom of the contour map represents the cavity and a color bar to the right gives the horizontal displacement values. Incremental horizontal displacement contours were used to determine the fracture initiation. Plots of length in the y-direction versus the total horizontal (x-direction) displacement were used to determine estimates of the effective crack length (L_{eff}) and the critical crack opening displacement (w_c). Both are determined from the point of fracture initiation to the borehole breakdown (peak) pressure (P_b). The origin of the contour plots of incremental horizontal displacement are at the center of the borehole, which was not captured in the image. The tip of the fracture is determined by the location where the horizontal displacements converge and a discontinuity in displacement is evident.

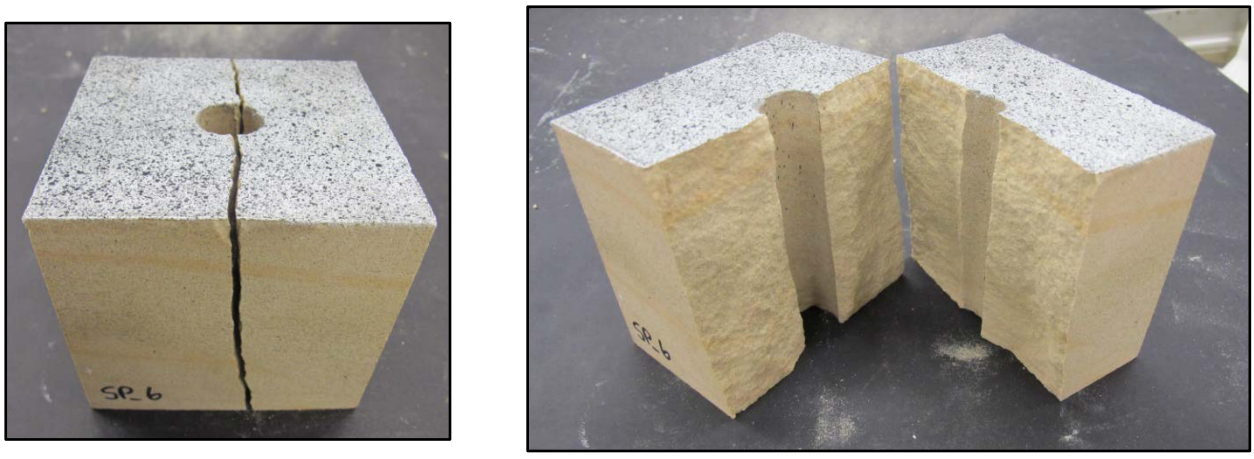

Figure 5: Images of Specimen 6 after failure from the cavity expansion test. The picture at the left shows the fracture going through the entire specimen where the far-field stress was applied in the direction of the fracture. The picture at the right shows the inside of the borehole and the face of the fracture plane.

As stated previously, the Kirsch solution and the Rankine failure criterion predict that the sum of the pressure in the borehole and the far-field should equal the tensile strength of the rock,

1.7 MPa. Figure 6 shows the results of the cavity expansion tests under different loading configurations. The borehole breakdown pressure was relatively consistent for the tests and did not change significantly with change of the far-field stress.

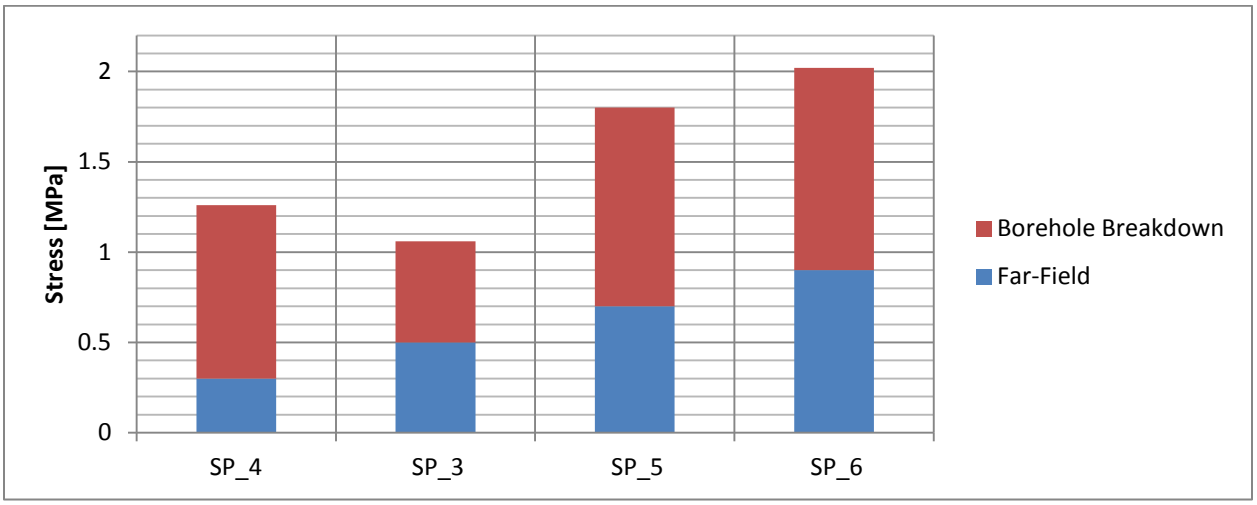

Figure 6: Bar chart of the relationship between the far-field stress and the borehole breakdown pressure for each of the specimens tested.

Specimen 3 of the cavity expansion tests was a Dunnville block subjected to a far-field stress of 0.3 MPa, or about 18 percent of the tensile strength. Fracture initiation was determined to be at about 60 percent of the breakdown pressure. The crack did not propagate in the y-direction (the direction of the far-field stress is applied) as a result of too small of a far-field stress because the difference between $\tilde{A}_1$ and $\tilde{A}_3$ (= 0) is not significant. At the peak pressure, the crack propagated out of the field of view, which meant the crack is longer than 20 mm.

Figure 7 illustrates displacement contours as the crack propagates while the pressure in the borehole steadily increased. Figure 7 shows the crack tip at 60 percent of peak pressure, and the fracture propagated almost through the entire specimen even though the crack initiated at about 50 percent of the peak pressure.

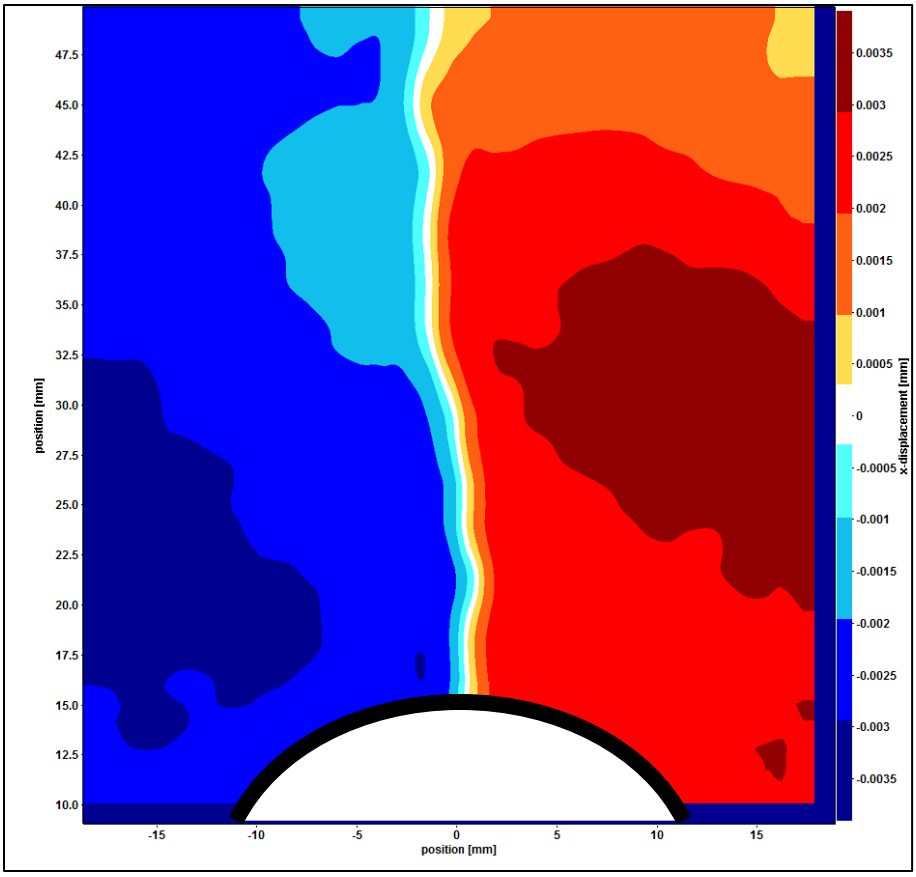

Figure 7: The incremental horizontal displacements of a SP_3 subjected to a far-field stress of 0.5 MPa between 40 – 60 % of the borehole breakdown pressure, P_b. The crack tip is at y = 45 mm.

Figure 8 shows a comparison of displacement contours for a Dunnville specimen subjected to a far-field stress of 0.7 MPa. Fracture initiation was determined to be about 35 percent of the peak pressure. The crack tip at 40 percent of failure pressure was located at about x = 30 mm, and at 50 percent of the peak pressure, at about x = 37 mm.

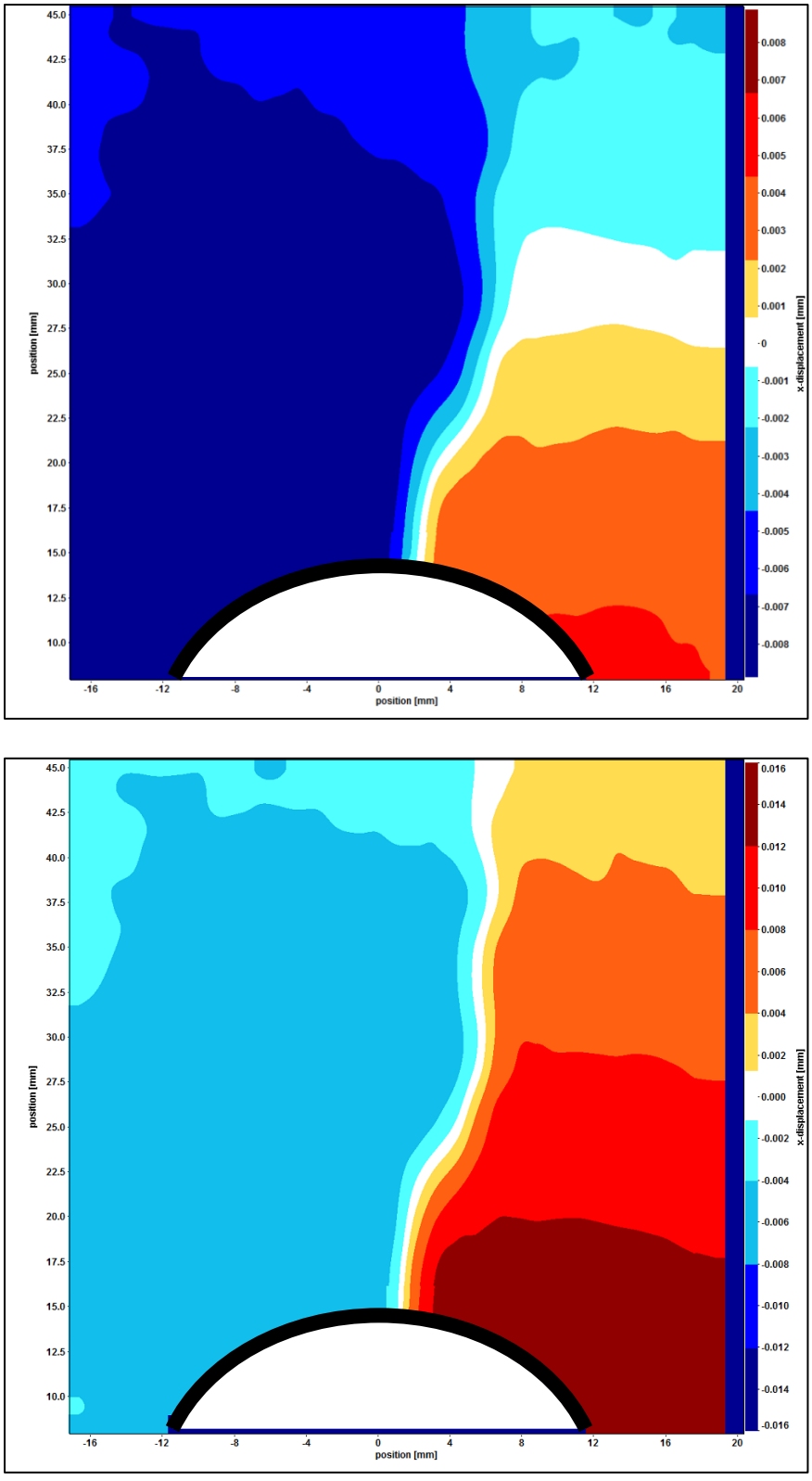

Figure 8: The incremental horizontal displacements of a SP_5 subjected to a far-field stress of 0.7 MPa between 20 – 40 % (top) and 20 - 50% (bottom) of the borehole breakdown pressure, P_b. The crack tip is at y = 30 mm (top) and then propagates to y = 37 mm (bottom).

Figures 9, 10 and 11 show the contour plots of the incremental horizontal displacement. The plots are from fracture initiation to the breakdown (peak) pressure. The fractures propagated through the entire specimen at peak pressure for all of the loading configurations.

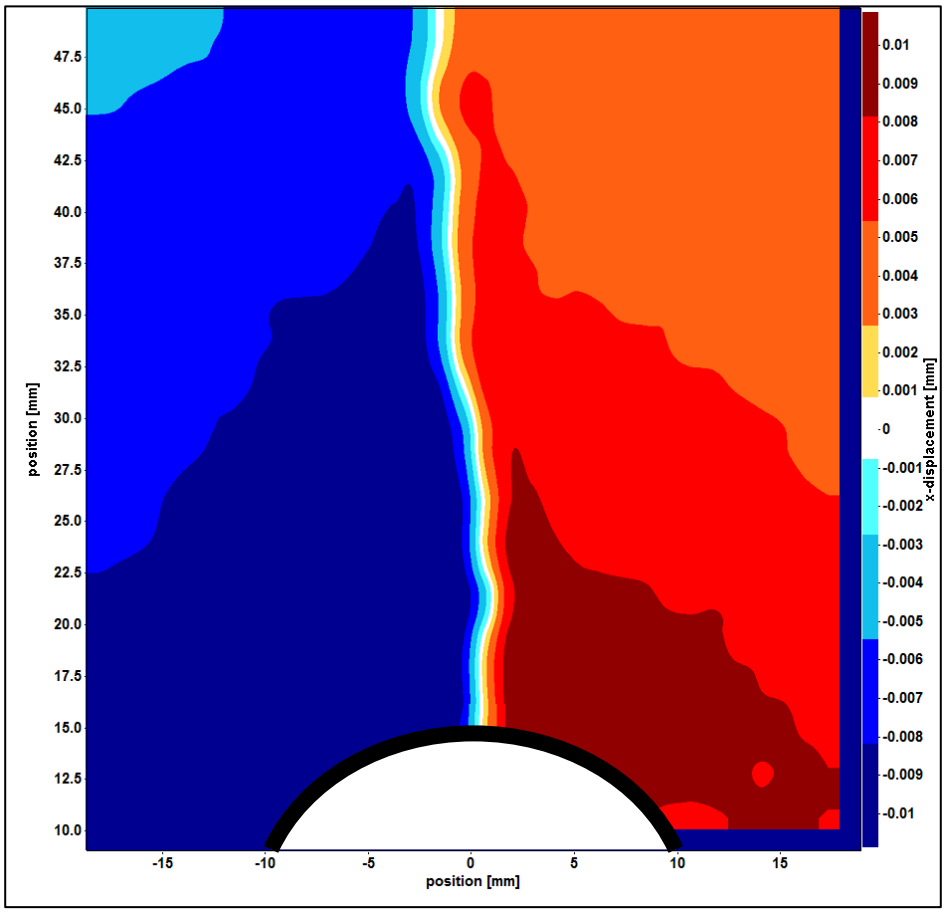

Figure 9: The incremental horizontal displacements of a SP_3 subjected to a far-field stress of 0.5 MPa between 60 – 100 % of the borehole breakdown pressure, P_b. The crack tip has propagated through the entire specimen.

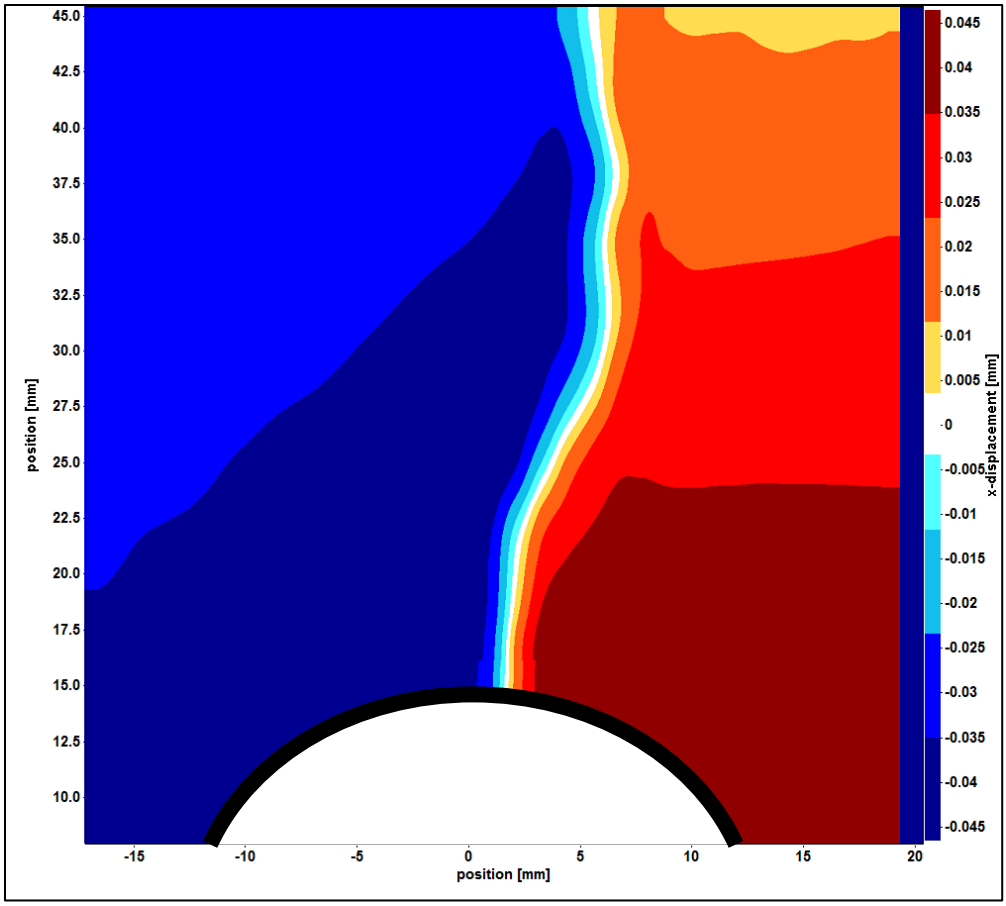

Figure 10: The incremental horizontal displacements of a SP_5 subjected to a far-field stress of 0.7 MPa between 40 – 100 % of the borehole breakdown pressure, P_b. The crack tip has propagated through the entire specimen.

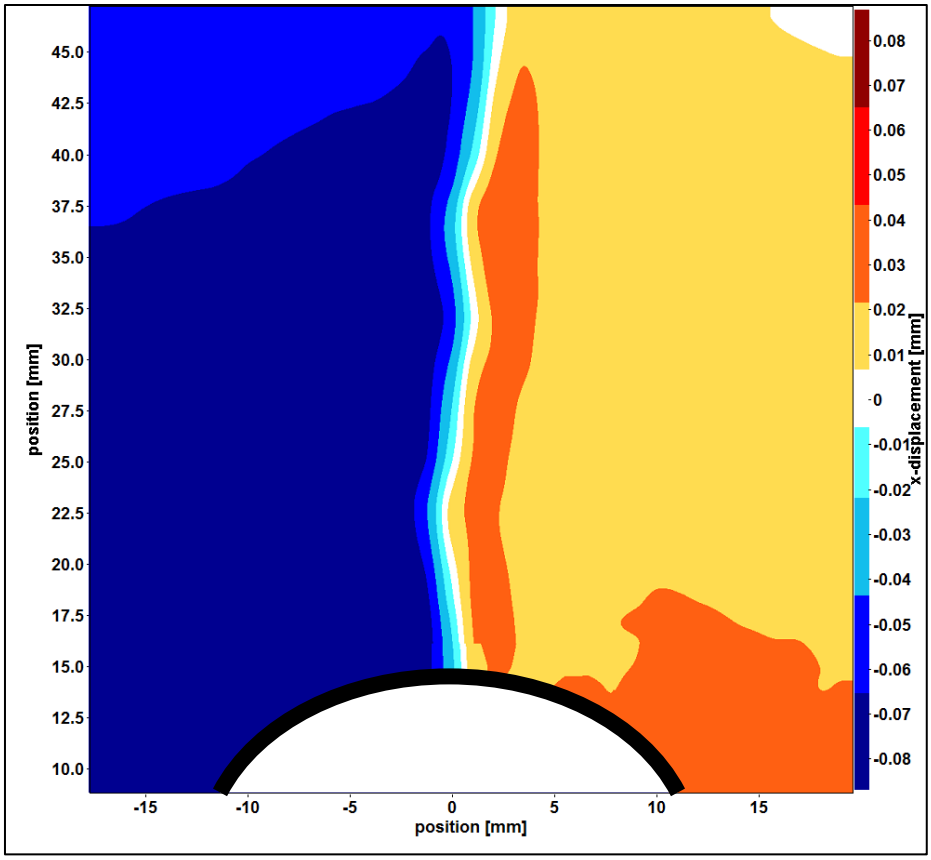

Figure 11: The incremental horizontal displacements of a specimen subjected to a far-field stress of 0.9 MPa between 30 – 90 % of the borehole breakdown pressure, P_b. The crack tip has propagated through the entire specimen.

Specimen	Far-Field		P_b	Initiation	w_c	L_{eff}
[-]	[MPa]	[% of $\tilde{A}_t$]	[MPa]	[% Peak]	[µm]	[mm]
SP_4	0.3	18	0.96	60	N/A	> 20
SP_3	0.5	29	0.56	50	N/A	>50
SP_5	0.7	41	1.10	35	83	>45
SP_6	0.9	53	1.12	30	109	>47

Table 1: Summary results from the specimens tested in relation to the far-field stresses applied. The effective crack length was determined at peak pressure.

5.0 Conclusions

Cavity expansion tests on Dunnville sandstone were performed with varying far-field stress. The fracture initiation pressure decreased as the far-field stress increased. It was found that the critical crack opening displacement increased as the far-field stress increased. The critical crack opening displacements in relation to far-field stresses of 0.7 and 0.9 MPa were 83-110 microns respectively. The fracture initiation pressure was found to be in the range of 30-60 percent of the peak pressure. A future research topic related to this project is determining the fracture toughness of the rock and the effect of applied stress.

6.0 References

Blanksma, D. Fracture Initiation near a Circular Cavity. M.S. thesis, University of Minnesota, 2013.

Hoek, E. Strength of jointed rock masses. Geotechnique, 33(3), 187-223, 1983.

Irwin, G. R. In Handbuch der Physik, Vol. 6, pp. 551-590. Springer, Berlin. 1958

Labuz, J. F., S. P. Shah, and C. H. Dowding. Experimental analysis of crack propagation in granite. International Journal of Rock Mechanics and Mining Sciences & Geomechanics Abstracts, 22(2), 1985.

Peters, W. H., & Ranson, W. F. Digital Imaging Techniques in Experimental Stess Analysis. Optical Engineering, 21(3), 427-31, 1982.

Zoback, M. D., F. Rummel, R. Jung, and C. B. Raleigh. Laboratory hydraulic fracturing experiments in intact and pre-fractured rock. In International Journal of Rock Mechanics and Mining Sciences & Geomechanics Abstracts, 14(2), 49-58, 1977.